

CERN-PH-EP-2012-189
03 July 2012

Measurement of the Cross Section for High- p_T Hadron Production in Scattering of 160 GeV/c Muons off Nucleons

The COMPASS Collaboration

Abstract

The cross section for production of charged hadrons with high transverse momenta in scattering of 160 GeV/c muons off nucleons at low photon virtualities has been measured at the COMPASS experiment at CERN. The results, which cover transverse momenta from 1.1 to 3.6 GeV/c, are compared to a next-to-leading order perturbative Quantum Chromodynamics (NLO pQCD) calculation in order to evaluate the applicability of pQCD to this process in the kinematic domain of the experiment. The shape of the calculated differential cross section as a function of transverse momentum is found to be in good agreement with the experimental data, but the normalization is underestimated by NLO pQCD. This discrepancy may point towards the relevance of terms beyond NLO in the pQCD framework. The dependence of the cross section on the pseudo-rapidity and on the charge of the hadrons is also discussed.

(to be submitted to Phys.Rev.Lett.)

The COMPASS Collaboration

C. Adolph⁸, M.G. Alekseev²⁴, V.Yu. Alexakhin⁷, Yu. Alexandrov^{15,*}, G.D. Alexeev⁷, A. Amoroso²⁷, A.A. Antonov⁷, A. Austregesilo^{10,17}, B. Badelek³⁰, F. Balestra²⁷, J. Barth⁴, G. Baum¹, Y. Bedfer²², J. Bernhard¹³, R. Bertini²⁷, M. Bettinelli¹⁶, K. Bicker^{10,17}, J. Bieling⁴, R. Birsa²⁴, J. Bisplinghoff³, P. Bordalo^{12,a}, F. Bradamante²⁵, C. Braun⁸, A. Bravar²⁴, A. Bressan²⁵, E. Burtin²², M. Chiosso²⁷, S.U. Chung¹⁷, A. Cicuttin²⁶, M.L. Crespo²⁶, S. Dalla Torre²⁴, S. Das⁶, S.S. Dasgupta⁶, S. Dasgupta⁶, O.Yu. Denisov²⁸, L. Dhara⁶, S.V. Donskov²¹, N. Doshita³², V. Duic²⁵, W. Dünneweber¹⁶, M. Dziewiecki³¹, A. Efremov⁷, C. Elia²⁵, P.D. Eversheim³, W. Eyrich⁸, M. Faessler¹⁶, A. Ferrero²², A. Filin²¹, M. Finger¹⁹, M. Finger jr.⁷, H. Fischer⁹, C. Franco¹², N. du Fresne von Hohenesche^{13,10}, J.M. Friedrich¹⁷, V. Frolov¹⁰, R. Garfagnini²⁷, F. Gautheron², O.P. Gavrichtchouk⁷, S. Gerassimov^{15,17}, R. Geyer¹⁶, M. Giorgi²⁵, I. Gnesi²⁷, B. Gobbo²⁴, S. Goertz⁴, S. Grabmüller¹⁷, A. Grasso²⁷, B. Grube¹⁷, R. Gushterski⁷, A. Guskov⁷, T. Guthörl^{9,b}, F. Haas¹⁷, D. von Harrach¹³, F.H. Heinsius⁹, F. Herrmann⁹, C. Heß², F. Hinterberger³, N. Horikawa^{18,c}, Ch. Höppner¹⁷, N. d'Hose²², S. Ishimoto^{32,d}, O. Ivanov⁷, Yu. Ivanshin⁷, T. Iwata³², R. Jahn³, V. Jary²⁰, P. Jasinski¹³, R. Joosten³, E. Kabuß¹³, D. Kang¹³, B. Ketzer¹⁷, G.V. Khaustov²¹, Yu.A. Khokhlov²¹, Yu. Kisselev², F. Klein⁴, K. Klimaszewski³⁰, S. Koblitz¹³, J.H. Koivuniemi², V.N. Kolosov²¹, K. Kondo³², K. Königsmann⁹, I. Konorov^{15,17}, V.F. Konstantinov²¹, A. Korzenev^{22,e}, A.M. Kotzinian²⁷, O. Kouznetsov^{7,22}, M. Krämer¹⁷, Z.V. Kroumchtein⁷, R. Kuhn¹⁷, F. Kunne²², K. Kurek³⁰, L. Lauser⁹, A.A. Lednev²¹, A. Lehmann⁸, S. Levorato²⁵, J. Lichtenstadt²³, T. Liska²⁰, A. Maggiora²⁸, A. Magnon²², N. Makke^{22,25}, G.K. Mallot¹⁰, A. Mann¹⁷, C. Marchand²², A. Martin²⁵, J. Marzec³¹, T. Matsuda¹⁴, G. Meshcheryakov⁷, W. Meyer², T. Michigami³², Yu.V. Mikhailov²¹, M.A. Moinester²³, A. Morreale^{22,f}, A. Mutter^{9,13}, A. Nagaytsev⁷, T. Nagel¹⁷, T. Negrini⁹, F. Nerling⁹, S. Neubert¹⁷, D. Neyret²², V.I. Nikolaenko²¹, W.-D. Nowak⁹, A.S. Nunes¹², A.G. Olshevsky⁷, M. Ostrick¹³, A. Padee³¹, R. Panknin⁴, D. Panzieri²⁹, B. Parsamyan²⁷, S. Paul¹⁷, E. Perevalova⁷, G. Pesaro²⁵, D.V. Peshekhonov⁷, G. Piragino²⁷, S. Platchkov²², J. Pochodzalla¹³, J. Polak^{11,25}, V.A. Polyakov²¹, J. Pretz^{4,g}, M. Quaresma¹², C. Quintans¹², J.-F. Rajotte¹⁶, S. Ramos^{12,a}, V. Rapatsky⁷, G. Reicherz², A. Richter⁸, E. Rocco¹⁰, E. Rondio³⁰, N.S. Rossiyskaya⁷, D.I. Ryabchikov²¹, V.D. Samoylenko²¹, A. Sandacz³⁰, M.G. Sapozhnikov⁷, S. Sarkar⁶, I.A. Savin⁷, G. Sbrizzai²⁵, P. Schiavon²⁵, C. Schill⁹, T. Schlüter¹⁶, K. Schmidt^{9,b}, L. Schmitt^{17,h}, K. Schönning¹⁰, S. Schopferer⁹, M. Schott¹⁰, W. Schröder⁸, O.Yu. Shevchenko⁷, L. Silva¹², L. Sinha⁶, A.N. Sissakian^{7,*}, M. Slunicka⁷, G.I. Smirnov⁷, S. Sosio²⁷, F. Sozzi²⁴, A. Srnka⁵, L. Steiger²⁴, M. Stolarski¹², M. Sulc¹¹, R. Sulej³⁰, P. Sznajder³⁰, S. Takekawa²⁸, J. Ter Wolbeek^{9,b}, S. Tessaro²⁴, F. Tessarotto²⁴, L.G. Tkatchev⁷, S. Uhl¹⁷, I. Uman¹⁶, M. Vandenbroucke²², M. Virius²⁰, N.V. Vlassov⁷, L. Wang², R. Windmolders⁴, W. Wiślicki³⁰, H. Wollny^{9,22,b}, K. Zaremba³¹, M. Zavertyaev¹⁵, E. Zemlyanichkina⁷, M. Ziembicki³¹, N. Zhuravlev⁷ and A. Zvyagin¹⁶

¹ Universität Bielefeld, Fakultät für Physik, 33501 Bielefeld, Germanyⁱ

² Universität Bochum, Institut für Experimentalphysik, 44780 Bochum, Germanyⁱ

³ Universität Bonn, Helmholtz-Institut für Strahlen- und Kernphysik, 53115 Bonn, Germanyⁱ

⁴ Universität Bonn, Physikalisches Institut, 53115 Bonn, Germanyⁱ

⁵ Institute of Scientific Instruments, AS CR, 61264 Brno, Czech Republic^j

⁶ Matrivani Institute of Experimental Research & Education, Calcutta-700 030, India^k

⁷ Joint Institute for Nuclear Research, 141980 Dubna, Moscow region, Russia^l

⁸ Universität Erlangen–Nürnberg, Physikalisches Institut, 91054 Erlangen, Germanyⁱ

⁹ Universität Freiburg, Physikalisches Institut, 79104 Freiburg, Germanyⁱ

¹⁰ CERN, 1211 Geneva 23, Switzerland

¹¹ Technical University in Liberec, 46117 Liberec, Czech Republic^j

¹² LIP, 1000-149 Lisbon, Portugal^m

¹³ Universität Mainz, Institut für Kernphysik, 55099 Mainz, Germanyⁱ

¹⁴ University of Miyazaki, Miyazaki 889-2192, Japanⁿ

- ¹⁵ Lebedev Physical Institute, 119991 Moscow, Russia
- ¹⁶ Ludwig-Maximilians-Universität München, Department für Physik, 80799 Munich, Germany^{io}
- ¹⁷ Technische Universität München, Physik Department, 85748 Garching, Germany^{io}
- ¹⁸ Nagoya University, 464 Nagoya, Japanⁿ
- ¹⁹ Charles University in Prague, Faculty of Mathematics and Physics, 18000 Prague, Czech Republic^j
- ²⁰ Czech Technical University in Prague, 16636 Prague, Czech Republic^j
- ²¹ State Research Center of the Russian Federation, Institute for High Energy Physics, 142281 Protvino, Russia
- ²² CEA IRFU/SPhN Saclay, 91191 Gif-sur-Yvette, France
- ²³ Tel Aviv University, School of Physics and Astronomy, 69978 Tel Aviv, Israel^p
- ²⁴ Trieste Section of INFN, 34127 Trieste, Italy
- ²⁵ University of Trieste, Department of Physics and Trieste Section of INFN, 34127 Trieste, Italy
- ²⁶ Abdus Salam ICTP and Trieste Section of INFN, 34127 Trieste, Italy
- ²⁷ University of Turin, Department of Physics and Torino Section of INFN, 10125 Turin, Italy
- ²⁸ Torino Section of INFN, 10125 Turin, Italy
- ²⁹ University of Eastern Piedmont, 15100 Alessandria, and Torino Section of INFN, 10125 Turin, Italy
- ³⁰ National Centre for Nuclear Research and University of Warsaw, 00-681 Warsaw, Poland^q
- ³¹ Warsaw University of Technology, Institute of Radioelectronics, 00-665 Warsaw, Poland^q
- ³² Yamagata University, Yamagata, 992-8510 Japanⁿ
- ^a Also at IST, Universidade Técnica de Lisboa, Lisbon, Portugal
- ^b Supported by the DFG Research Training Group Programme 1102 “Physics at Hadron Accelerators”
- ^c Also at Chubu University, Kasugai, Aichi, 487-8501 Japanⁿ
- ^d Also at KEK, 1-1 Oho, Tsukuba, Ibaraki, 305-0801 Japan
- ^e On leave of absence from JINR Dubna
- ^f present address: National Science Foundation, 4201 Wilson Boulevard, Arlington
- ^g present address: III. Physikalisches Institut, RWTH Aachen University, 52056 Aachen
- ^h Also at GSI mbH, Planckstr. 1, D-64291 Darmstadt, Germany
- ⁱ Supported by the German Bundesministerium für Bildung und Forschung
- ^j Supported by Czech Republic MEYS grants ME492 and LA242
- ^k Supported by SAIL (CSR), Govt. of India
- ^l Supported by CERN-RFBR grants 08-02-91009
- ^m Supported by the Portuguese FCT - Fundação para a Ciência e Tecnologia, COMPETE and QREN, grants CERN/FP/109323/2009, CERN/FP/116376/2010 and CERN/FP/123600/2011
- ⁿ Supported by the MEXT and the JSPS under the Grants No.18002006, No.20540299 and No.18540281; Daiko Foundation and Yamada Foundation
- ^o Supported by the DFG cluster of excellence ‘Origin and Structure of the Universe’ (www.universe-cluster.de)
- ^p Supported by the Israel Science Foundation, founded by the Israel Academy of Sciences and Humanities
- ^q Supported by Polish NCN grant DEC-2011/01/M/ST2/02350
- * Deceased

Most of the current knowledge about the structure of the nucleon has been derived from high-energy lepton-nucleon scattering experiments [1]. The theoretical framework for the interpretation of data from such experiments is perturbative Quantum Chromodynamics (pQCD). In the presence of a large momentum transfer in the reaction, pQCD relies on the collinear factorization of the cross section into non-perturbative collinear parton distribution functions (PDFs), hard partonic scattering cross sections calculable in perturbation theory, and non-perturbative collinear fragmentation functions (FFs) [2]. This Letter discusses the measurement of the cross section for production of charged hadrons with high transverse momenta p_T in muon-nucleon (μ - N) scattering at low photon virtualities, $\mu N \rightarrow \mu' h^\pm X$. In the pQCD framework, the lowest-order contributions to this reaction are (1) photon-gluon fusion (PGF), in which a virtual photon emitted by the lepton interacts with a gluon inside the nucleon via the formation of a quark-antiquark pair, $\gamma g \rightarrow q\bar{q}$, (2) QCD Compton (QCDC) scattering, in which the photon interacts with a quark in the nucleon leading to the emission of a hard gluon, $\gamma q \rightarrow qg$, and (3) numerous resolved-photon processes, in which the photon fluctuates into a virtual vector-meson-like state before it interacts with the nucleon.

The ability of pQCD to correctly describe high- p_T hadron production can be evaluated by comparing the calculated cross section to the experimentally measured one. This benchmark is sensitive to the accuracy, with which the partonic cross section can be calculated in perturbation theory, as well as to the validity of collinear factorization itself. For inclusive high- p_T hadron or jet production in proton-proton (p - p) scattering, cross sections have been measured at FNAL [3, 4, 5], CERN [6] and BNL [7, 8, 9, 10, 11, 12] at center-of-mass system (CMS) energies $\sqrt{s_{p-p}}$ from 20 GeV to 200 GeV. The comparison of these data to next-to-leading order (NLO) pQCD calculations [13] shows that while there is good agreement at $\sqrt{s_{p-p}} = 200$ GeV (RHIC), the theory increasingly underestimates the cross sections with decreasing $\sqrt{s_{p-p}}$. The disagreement reaches up to an order of magnitude at 20 GeV. These discrepancies can be reconciled by the inclusion of all-order resummations of threshold logarithms [14], which are related to soft gluon emissions and are usually performed up to next-to-leading logarithmic (NLL) accuracy.

The electromagnetic probe in muon-lepton scattering has the advantage over p - p scattering that the kinematics of the reaction is better known since the momentum and energy transfers to the nucleon can be measured for each event by analyzing the scattered lepton. In the regime of quasi-real photoproduction, i.e. at low photon virtualities Q^2 , the cross section for high- p_T hadron production in lepton-nucleon scattering can be calculated in NLO pQCD via the Weizsäcker-Williams formalism [15, 16]. For dijet production at HERA at very high photon-nucleon CMS energies $142 \leq W_{\gamma N} \leq 293$ GeV, the NLO pQCD results agree well with the experimental data [17]. At the energy of fixed-target experiments, such a check of the applicability of pQCD to high- p_T particle production at low Q^2 has not been done yet. The cross section for high- p_T hadron production in the scattering of 28 GeV/ c positrons off nucleons has been published by the HERMES Collaboration [18]. However, the measurement hardly exceeds p_T values of 2 GeV/ c , which sets rather low factorization and renormalization scales for pQCD calculations, and a comparison to NLO pQCD was not attempted. In this Letter, the measurement of the cross section for production of unidentified charged hadrons with high p_T in scattering of 160 GeV/ c muons off nucleons (CMS energy $\sqrt{s_{\mu-N}} = 17.4$ GeV) at the COMPASS experiment [19] at low photon virtualities is presented. The cross section for this kinematic domain has been calculated in NLO pQCD [20].

The hadron-production cross section is measured in bins of p_T and η of widths Δp_T and $\Delta\eta$, respectively, and is defined as

$$E \frac{d^3\sigma}{dp^3} = \frac{1}{2\pi p_T \Delta p_T \cdot \Delta\eta \cdot L \cdot \varepsilon} N_h, \quad (1)$$

where E and p are energy and momentum of the hadron, respectively, $p_T = p \cdot \sin\theta$ is the transverse momentum of the hadron with respect to the direction of the virtual photon (θ is the angle between the virtual photon and the hadron momenta), and $\eta = -\ln \tan(\theta/2)$ is the pseudo-rapidity of the hadron, all measured in the laboratory system. The integrated luminosity is denoted by L , N_h is the number of observed hadrons in a given bin of p_T and η , and ε is the acceptance-correction factor, which is determined

independently for both hadron charges for each bin of p_T and η . This factor corrects the number of observed hadrons for geometrical acceptance and detection efficiency of the spectrometer as well as for kinematic smearing. The cross section is defined as a single-inclusive cross section, i.e. several high- p_T hadrons per muon-scattering event are counted for the hadron yield N_h .

The experimental data were recorded in 2004 with the COMPASS spectrometer at CERN. In the experiment, a naturally-polarized 160 GeV/c μ^+ -beam scatters off a polarized, isoscalar target that consists of granulated ^6LiD immersed in liquid helium. The small admixtures of H, ^3He , and ^7Li lead to an excess of neutrons of about 0.1%. The target is arranged in two oppositely polarized 60 cm long cells. The unpolarized cross section is obtained by averaging over the target polarizations. Since the azimuthal angles of the produced hadrons are integrated over, the cross section does not depend on the beam polarization. The integrated luminosity is determined via the direct measurement of the rate of beam muons crossing the target and is found to be equal to $142 \text{ pb}^{-1} \pm 10\%$ (syst.) after correction for the dead time of the data acquisition system. As an independent cross check of the luminosity, the structure function of the nucleon F_2 is determined from this data set and compared to the NMC parametrization of F_2 [21] yielding satisfactory agreement [22]. The high- p_T analysis is based on events that were recorded by the quasi-real photoproduction trigger systems [23]. These triggers are based on the coincidence between the detection of the scattered muon at low scattering angles and an energy deposit exceeding about 5 GeV in one of the two hadronic calorimeters, to suppress background from muon-electron scattering and radiative elastic or quasi-elastic muon-scattering events. Events are accepted if the photon virtuality $Q^2 < 0.1 \text{ (GeV/c)}^2$ and if the fractional energy transferred from the incident muon to the virtual photon is in the range $0.2 \leq y \leq 0.8$, where the acceptance of the trigger systems is largest. These selections result in the energy range $7.8 \leq W_{\gamma N} \leq 15.5 \text{ GeV}$. The fraction of the virtual-photon energy transferred to the hadron h^\pm is constrained by $0.2 \leq z \leq 0.8$. Moreover, hadrons are required to have momenta $p \geq 15 \text{ GeV/c}$ to ensure full trigger efficiency. The angle of the hadron with respect to the direction of the virtual photon has to be in the range $10 \leq \theta \leq 120 \text{ mrad}$, which corresponds to a range of muon-nucleon CMS pseudo-rapidities $2.4 \geq \eta_{\text{CMS}} \geq -0.1$. In addition to these *kinematic* criteria, the selection of reconstructed hadrons is subject to several *geometrical* cuts: the positions of the muon-scattering vertices are limited to the fiducial target volume, the hadron tracks must not cross the solenoid magnet of the polarized target, and the hadron tracks must hit one of the two hadronic calorimeters, excluding 3 cm wide margins around the edges (for full trigger efficiency).

The acceptance correction factors of Eq. (1) are determined with a Monte-Carlo (MC) simulation of μ - N scattering in the COMPASS experiment. Events are generated with PYTHIA6 [24], the response of the spectrometer is simulated with a GEANT3-based program [25], and the data are reconstructed with the same software as the experimental data [19]. The acceptance factor for the bin $p_T \in [p_{T,1}, p_{T,2}]$ is defined as

$$\varepsilon = \frac{N^{\text{rec}}(p_T^{\text{rec}} \in [p_{T,1}, p_{T,2}])}{N^{\text{gen}}(p_T^{\text{gen}} \in [p_{T,1}, p_{T,2}])} \quad , \quad (2)$$

where N^{rec} is the number of reconstructed hadrons in the bin of reconstructed transverse momentum p_T^{rec} , and N^{gen} is the number of generated hadrons in the MC sample in the bin of generated transverse momentum p_T^{gen} . While both, N^{rec} and N^{gen} are subject to the above-listed *kinematic* selection criteria, the *geometrical* cuts are only applied to N^{rec} so that the loss of hadrons due to these cuts is accounted for by the acceptance correction.

Hadrons that are created at the μ - N vertex constitute the signal of the measurement and have to be separated from background hadrons, which are created in secondary interactions of other hadrons in the target material. This separation is performed by the vertex-reconstruction algorithm, which is however impaired by the fact that the angle between the incoming and outgoing muon tracks is very small at low Q^2 . The background contamination can not be estimated directly from the MC data, because simulations with the two hadron-shower models available in GEANT3 (GHEISHA and FLUKA) give inconsistent results. Hence the background contribution is determined in each p_T bin from the experimental data by

fitting the shape of the distribution of position differences between two-particle vertices formed by the incoming muon track and the outgoing muon track on the one hand, and the incoming muon track and the outgoing hadron track on the other hand [26]. The distribution for signal hadrons, originating from the same interaction as the outgoing muon track, has a symmetric shape, while for background hadrons there is a characteristic asymmetric shape. The results of these fits show that the background contribution to the experimental data is consistent with zero. However, cross checks with both MC data sets indicate that the background contribution can be systematically underestimated by 6% using this method. In addition, the described procedure is statistically limited for the highest p_T bins because there are too few entries in the vertex-difference distributions to exclude a non-zero background contribution with high statistical accuracy. For the four highest p_T bins, the background level p_{excl} at which a non-zero background contribution can be excluded at 90% confidence level is greater than 6%. Therefore, the possible contribution of residual background to the hadron yield is conservatively estimated to be $2 \times 6\%$ for the six lowest p_T bins and $p_{\text{excl}} + 6\%$ for the four highest p_T bins. These values are used as systematic uncertainties of the acceptance factors.

A second contribution to the systematic uncertainties of the acceptance factors arises from the fact that they are determined in a one-dimensional way, i.e. by integrating over all kinematic variables other than p_T . The resulting uncertainty is quantified by calculating the acceptance correction binned in two variables, i.e. p_T and one of the variables Q^2 , y , x_{Bj} (Bjorken scaling variable), $W_{\gamma N}$, z , θ . A comparison of the cross section calculated in two variables, summed up over the second variable, with the one-dimensional result yields deviations below 3%. This uncertainty is added in quadrature to the uncertainties from background contamination, resulting in the following definition of the upper (ϵ_u) and lower (ϵ_d) limits of the systematic error band of the acceptance factors

$$\begin{aligned}\epsilon_u &= \epsilon \cdot \left(1 + \sqrt{0.03^2 + (0.06 + \max(0.06, p_{\text{excl}}))^2} \right) \\ \epsilon_d &= \epsilon \cdot (1 - 0.03) \quad .\end{aligned}$$

Another systematic uncertainty of the cross section is the 10% normalization uncertainty from the luminosity determination.

The cross section for production of charged high- p_T hadrons in μ - N scattering at $Q^2 < 0.1$ (GeV/c)² and $\sqrt{s_{\mu-N}} = 17.4$ GeV, integrated over the full kinematic range, is presented in Fig. 1 and listed in Tab. 1. The presented cross section is not corrected for QED radiative effects. The discrete p_T values at which the cross section values from the binned analysis of Eq. (1) are drawn are calculated using the method of Lafferty & Wyatt [28] and are denoted by $\langle p_T \rangle_{\text{lw}}$ in Tab. 1. The cross section drops by about four orders of magnitude over the measured p_T range. The only apparent deviation from an exponential shape is a slight hardening of the spectrum at about $p_T = 2.5$ GeV/c. In Fig. 1, the data are compared to the NLO pQCD calculation of Ref. [20], which has been updated [27] to implement the above-stated kinematic selections and the DSS FFs [29] for unidentified charged hadrons. The three curves correspond to different choices of the renormalization (μ_r) and factorization (μ_f) scales in the pQCD calculation. The standard choice for the scales in pQCD is $\mu = \mu_r = \mu_f = p_T$ and the scale uncertainty is estimated by varying the scale in the range $2p_T \geq \mu \geq p_T/2$. For $p_T \gtrsim 1.75$ GeV/c, the pQCD result at the standard scale $\mu = p_T$ underestimates the experimental cross section by a factor of three to four, but follows the shape of the differential cross section remarkably well. For $p_T \lesssim 1.75$ GeV/c the pQCD results should be discussed and interpreted very cautiously, because the factorization of the calculated cross section is expected to break down when reaching small scales μ . The large scale uncertainty of the cross section shows that contributions beyond NLO are likely to be significant in the pQCD framework. The analogy to p - p scattering at low CMS energies suggests that all-order resummations of threshold logarithms, once available, might reconcile the normalization discrepancy.

In Fig. 2, the p_T dependence of the experimental cross section is presented in bins of η_{CMS} , together with the comparison to NLO pQCD. The steeper p_T slopes of the cross section at forward rapidities as compared to central rapidity are well described by the pQCD curves, and the normalization difference

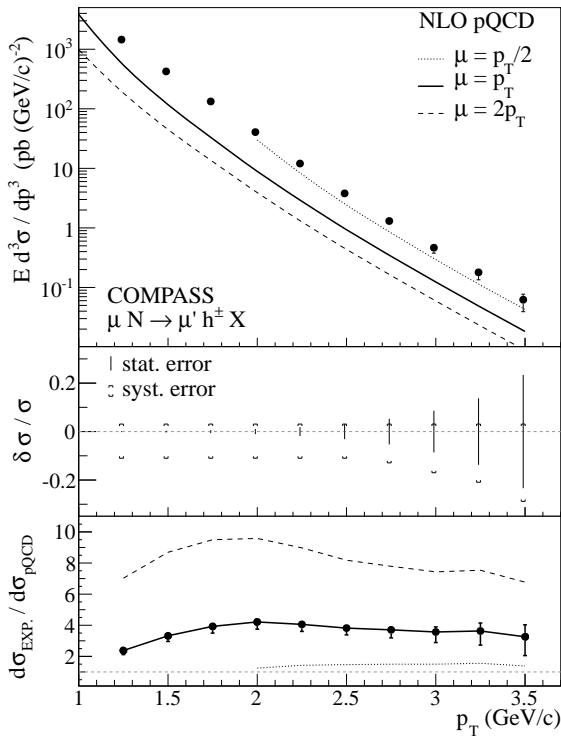


Fig. 1: Cross section for high- p_T hadron production in μ - N scattering, integrated over the full kinematic range (see text). The data are compared to the NLO pQCD calculation [20, 27]. The error bars in the upper panel are the quadratic sums of statistical and systematic uncertainties. The middle panel shows the relative statistical and systematic uncertainties of the measurement. The normalization uncertainty of 10% from the luminosity measurement is not shown. The lower panel shows the ratio of the measured over calculated cross sections.

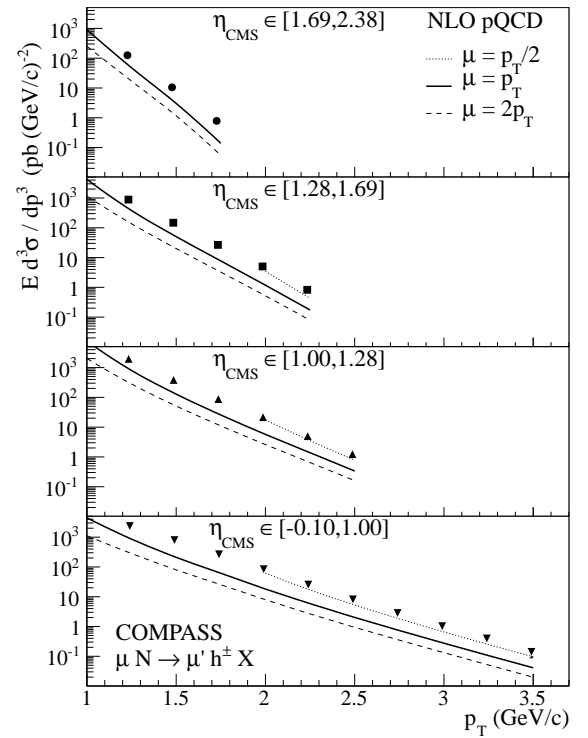


Fig. 2: Cross section in bins of η_{CMS} . The data are compared to the NLO pQCD calculation. The error bars are the quadratic sums of statistical and systematic uncertainties. The normalization uncertainty of 10% from the luminosity measurement is not shown.

between the theoretical calculation ($\mu = p_T$) and the experimental values remains about the same for all rapidities. This is a positive indication for the consistency of the pQCD results.

The charge ratio of the cross sections for the production of negatively over positively charged hadrons is displayed in Fig. 3. No strong p_T dependence is observed within the statistical accuracy of the measurement. The charge ratio is sensitive to the contributions of the different partonic processes to the cross section. The QCDC process can lead to an excess of positively charged hadrons because the electromagnetic coupling to u quarks is four times larger than to d quarks, and u quarks are more likely to produce positively charged mesons. The PGF process, on the other hand, is not expected to result in a charge asymmetry, assuming independent quark fragmentation. The NLO pQCD calculation, also shown in Fig. 3, features a charge ratio of about unity for $p_T = 1 \text{ GeV}/c$ and a clear decrease with increasing p_T , in disagreement with the data.

In summary, the single-inclusive cross section for charged-hadron production in μ - N scattering at $\sqrt{s_{\mu-N}} = 17.4 \text{ GeV}$ was measured for photon virtualities $Q^2 < 0.1 \text{ (GeV}/c)^2$ in the η_{CMS} interval between -0.1 and 2.4 and for transverse hadron momenta up to $3.6 \text{ GeV}/c$. While the shape of the measured p_T -differential cross section agrees well with NLO pQCD over the full rapidity range, the present theoretical calculation underestimates the experimental cross section by a factor of three to four. Thus, the pQCD calculation at

NLO appears to be insufficient to fully describe high- p_T hadron production in μ - N scattering at low Q^2 in the kinematic domain of COMPASS. The resummation of threshold logarithms beyond NLO might help to resolve this discrepancy. Once an agreement with the measured cross section has been established, the pQCD framework can be employed to constrain the polarization of gluons in the nucleon [20], using the double-spin asymmetry of single high- p_T hadron production at low Q^2 extracted from the full COMPASS muon-scattering data set. This approach is complementary to previous measurements of the gluon polarization by COMPASS using polarized high- p_T hadron-pair production [30, 31], which employ the MC generators PYTHIA and LEPTO [32], respectively, to quantify the contribution of PGF to the cross section.

We thank Werner Vogelsang for many useful discussions and for providing the updated NLO pQCD calculation. We acknowledge the support of the CERN management and staff, as well as the skills and efforts of the technicians of the collaborating institutions. Special thanks go to V. Anosov and V. Pesaro for their technical support during the installation and the running of this experiment. This work was made possible thanks to the financial support of our funding agencies.

References

- [1] A. W. Thomas and W. Weise, , “The Structure of the Nucleon”, Wiley-VCH, 2001.
- [2] G. Sterman *et al.*, *Rev.Mod.Phys.* **67** (1995) 157–248.
- [3] G. Donaldson, H. Gordon, K.-W. Lai, I. Stumer, A. Barnes *et al.*, *Phys.Lett.* **B73** (1978) 375.
- [4] FNAL E704 Collaboration, D. Adams *et al.*, *Phys.Rev.* **D53** (1996) 4747–4755.
- [5] FNAL E706 Collaboration, L. Apanasevich *et al.*, *Phys.Rev.* **D68** (2003) 052001, [arXiv:hep-ex/0204031](#) [hep-ex].
- [6] D. Lloyd Owen *et al.*, *Phys.Rev.Lett.* **45** (1980) 89.
- [7] PHENIX Collaboration, S. Adler *et al.*, *Phys.Rev.Lett.* **91** (2003) 241803, [arXiv:hep-ex/0304038](#) [hep-ex].
- [8] STAR Collaboration, B. Abelev *et al.*, *Phys.Rev.Lett.* **97** (2006) 252001, [arXiv:hep-ex/0608030](#) [hep-ex].
- [9] STAR Collaboration, J. Adams *et al.*, *Phys.Lett.* **B637** (2006) 161–169, [arXiv:nucl-ex/0601033](#) [nucl-ex].
- [10] PHENIX Collaboration, A. Adare *et al.*, *Phys.Rev.* **D79** (2009) 012003, [arXiv:0810.0701](#) [hep-ex].

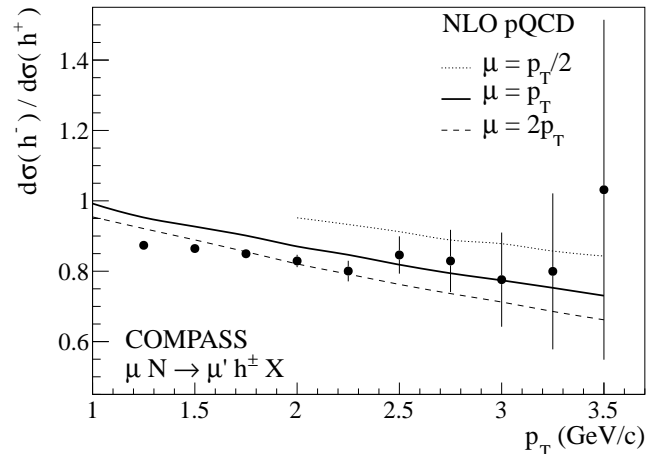


Fig. 3: Ratio of cross sections for production of h^- over h^+ . The data are compared to the NLO pQCD calculation. The error bars are statistical.

- [11] STAR Collaboration, B. Abelev *et al.*, *Phys.Rev.* **D80** (2009) 111108, arXiv:0911.2773 [hep-ex].
- [12] PHENIX Collaboration, A. Adare *et al.*, *Phys.Rev.* **C83** (2011) 064903, arXiv:1102.0753 [nucl-ex].
- [13] C. Bourrely and J. Soffer, *Eur.Phys.J.* **C36** (2004) 371–374, arXiv:hep-ph/0311110.
- [14] D. de Florian and W. Vogelsang, *Phys.Rev.* **D71** (2005) 114004, arXiv:hep-ph/0501258.
- [15] S. Frixione, M. L. Mangano, P. Nason and G. Ridolfi, *Phys.Lett.* **B319** (1993) 339–345, arXiv:hep-ph/9310350 [hep-ph].
- [16] D. de Florian and S. Frixione, *Phys.Lett.* **B457** (1999) 236–244, arXiv:hep-ph/9904320 [hep-ph].
- [17] ZEUS Collaboration, S. Chekanov *et al.*, *Phys.Rev.* **D76** (2007) 072011, arXiv:0706.3809 [hep-ex].
- [18] HERMES Collaboration, A. Airapetian *et al.*, *JHEP* **1008** (2010) 130, arXiv:1002.3921 [hep-ex].
- [19] COMPASS Collaboration, P. Abbon *et al.*, *Nucl.Instrum.Meth.* **A577** (2007) 455–518.
- [20] B. Jäger, M. Stratmann and W. Vogelsang, *Eur.Phys.J.* **C44** (2005) 533–543, arXiv:hep-ph/0505157.
- [21] NMC Collaboration, M. Arneodo *et al.*, *Phys.Lett.* **B364** (1995) 107–115, arXiv:hep-ph/9509406 [hep-ph].
- [22] COMPASS Collaboration, C. Höppner *et al.*, *Proceedings of SPIN Praha 2010* (2011), arXiv:hep-ph/1104.2926.
- [23] C. Bernet *et al.*, *Nucl.Instrum.Meth.* **A550** (2005) 217–240.
- [24] T. Sjostrand *et al.*, *Comput.Phys.Commun.* **135** (2001) 238–259, arXiv:hep-ph/0010017.
- [25] R. Brun *et al.*, *CERN Program Library Long Writeup W5013* (1993).
- [26] C. Höppner, PhD thesis, Technische Universität München, CERN-THESIS-2012-005 (2012).
- [27] W. Vogelsang. Private communication, 2012.
- [28] G. Lafferty and T. Wyatt, *Nucl.Instrum.Meth.* **A355** (1995) 541–547.
- [29] D. de Florian, R. Sassot and M. Stratmann, *Phys.Rev.* **D75** (2007) 114010, arXiv:hep-ph/0703242.
- [30] COMPASS Collaboration, E. Ageev *et al.*, *Phys.Lett.* **B633** (2006) 25–32, arXiv:hep-ex/0511028 [hep-ex].
- [31] COMPASS Collaboration, C. Adolph *et al.*, *submitted to Phys.Lett.* **B** (2012), arXiv:1202.4064 [hep-ph].
- [32] G. Ingelman *et al.*, *Comput.Phys.Commun.* **101** (1997) 108–134, arXiv:hep-ph/9605286.

Table 1: Measured cross section for high- p_T hadron production in μ - N scattering at $\sqrt{s_{\mu-N}} = 17.4$ GeV. The cross section is integrated over the full kinematic range defined in the text. The columns show: (1) p_T range of the bin; (2) p_T value of data point in Fig. 1; (3) differential cross section summed over hadron charges (please note that there is an additional 10% normalization uncertainty from luminosity); and (4) charge ratio of the cross section.

$[p_{T,1}, p_{T,2}]$ (GeV/c)	$\langle p_T \rangle_{lw}$ (GeV/c)	$\frac{d\sigma}{dp_T} = \frac{1}{p_{T,2}-p_{T,1}} \int_{p_{T,1}}^{p_{T,2}} \frac{d\sigma}{dp_T} dp_T$ (pb(GeV/c) $^{-1}$)	$\frac{d\sigma}{dp_T} (h^-) / \frac{d\sigma}{dp_T} (h^+)$
[1.125, 1.375]	1.239	$[2.810 \pm 0.006$ (stat.) $^{+0.087}_{-0.310}$ (syst.)] $\cdot 10^4$	0.874 ± 0.004 (stat.)
[1.375, 1.625]	1.489	$[9.87 \pm 0.04$ (stat.) $^{+0.31}_{-1.09}$ (syst.)] $\cdot 10^3$	0.864 ± 0.007 (stat.)
[1.625, 1.875]	1.739	3603 ± 23 (stat.) $^{+112}_{-397}$ (syst.)	0.850 ± 0.011 (stat.)
[1.875, 2.125]	1.989	1261 ± 14 (stat.) $^{+40}_{-139}$ (syst.)	0.829 ± 0.018 (stat.)
[2.125, 2.375]	2.239	421 ± 8 (stat.) $^{+14}_{-47}$ (syst.)	0.800 ± 0.030 (stat.)
[2.375, 2.625]	2.489	148 ± 5 (stat.) $^{+5}_{-17}$ (syst.)	0.85 ± 0.06 (stat.)
[2.625, 2.875]	2.739	55.9 ± 3.0 (stat.) $^{+1.8}_{-7.3}$ (syst.)	0.83 ± 0.09 (stat.)
[2.875, 3.125]	2.989	21.7 ± 1.9 (stat.) $^{+0.7}_{-3.7}$ (syst.)	0.78 ± 0.14 (stat.)
[3.125, 3.375]	3.239	9.08 ± 1.25 (stat.) $^{+0.29}_{-1.90}$ (syst.)	0.80 ± 0.23 (stat.)
[3.375, 3.625]	3.490	3.40 ± 0.80 (stat.) $^{+0.11}_{-0.98}$ (syst.)	1.0 ± 0.5 (stat.)